

A Class of OFT Controllers for Torque-Saturated Robot Manipulators: Lyapunov Stability and Experimental Evaluation

Javier Moreno-Valenzuela · Víctor Santibáñez · Ricardo Campa

Received: 12 March 2007 / Accepted: 26 August 2007 /
Published online: 29 September 2007
© Springer Science + Business Media B.V. 2007

Abstract The trajectory tracking of robot manipulators is addressed in this paper. Two important practical situations are considered: the fact that robot actuators have limited power, and that only position measurements are carried out. Let us notice that a few solutions for the torque-bounded OFT (output feedback tracking) control has been proposed. In this paper we contribute to this subject by presenting a class of OFT controllers for torque-constrained robots. The theory of singularly perturbed systems is crucial in the analysis of the closed-loop system trajectories. As a second contribution of this paper, we present a detailed experimental study of six control schemes, which were tested in a two degrees-of-freedom direct-drive robot, confirming the advantages of the proposed methodology.

Keywords Tracking control · Unmeasurable joint velocity · Robot manipulator · Lyapunov theory · Direct-drive robot

1 Introduction

Physical systems are subject to power limitations. For actuator-driven mechanisms, such as robots, this fact shows up in the form of joint saturation constraints, which may degrade the efficiency of the entire system. Therefore, when designing control

J. Moreno-Valenzuela (✉)
Centro de Investigación y Desarrollo de Tecnología Digital del IPN,
CITEDI-IPN, Ave. del Parque 1310, Mesa de Otay, Tijuana, B.C. 22510, Mexico
e-mail: moreno@citedi.mx

V. Santibáñez · R. Campa
Instituto Tecnológico de La Laguna, Apdo. Postal 49 Adm. 1, Torreón, Coah. 27001, Mexico
e-mail: vsantiba@itlaguna.edu.mx

R. Campa
e-mail: recampa@itlaguna.edu.mx

strategies for such mechanisms, it is important to take into account those actuator limits. Some recent books (e.g., [8–10]) and papers deal with this topic.

With respect to robot manipulators, most of the controllers that take into account the problem of bounded torque inputs have been targeted at the full-state feedback set-point control problem. For example, in Zergeroglu et al. [29], two model-based control schemes to solve the set-point control problem of n -link robotic manipulators with amplitude-limited control inputs were proposed. In Meza et al. [16], a novel passivity-based saturated nonlinear configuration of a PID regulator was introduced. The work by Zavala-Río and Santibáñez [26, 27], dealt with extensions of the PD-with-gravity-compensation control law assuring joint position regulation in robots constrained to bounded torques. Another approach was proposed in Dixon [7], where an amplitude-limited torque input controller for revolute robot manipulators with uncertainty in the kinematic and dynamic models was introduced. The cited references show that in order to study the regulation problem of robots subject to input saturation, a complex stability analysis is necessary. The analysis becomes much more complicated in the case of OFT (output feedback tracking) control of manipulators subject to constrained torques. Let us notice that to overcome the situation of noisy velocity and acceleration measurements, an OFT controller (which estimates those signals from position measurements) can be used to guarantee the motion control.

From a literature review, it seems that no much effort has been focused in studying the more general problem of OFT control of manipulators subject to constrained torques. The paper by Lee and Khalil [13] presents an adaptive OFT tracking controller for which local ultimately boundedness of the error signal is shown. The boundedness of the control signals in [13] is assured by limiting the control law with a saturation function and assuming that error signals are always inside a region where the produced torque is limited. Another result was proposed by Loría and Nijmeijer [15], where it is shown how the semiglobal and exponential stabilization of the closed-loop system is achieved by using large enough observer gains, while bounded controls are guaranteed. In the papers by Dixon et al. [4, 5], a controller is proposed to solve the OFT control with bounded torques, which yielded semiglobal stability in closed-loop. More recently, Santibáñez and Kelly [23] presented a torque-bounded controller by assuming that viscous friction is present at the robot joints, then the global asymptotic stability is assured if large enough viscous friction damping is present.

It is noteworthy that other results on OFT control of manipulators have been proposed more recently, including robust versions, [1, 6, 17, 28], but none of these addressed the case of actuator limited power.

In this paper, a general methodology to design torque-bounded OFT controllers is introduced. We have invoked the theory of singularly perturbed systems [12] and the concept of the energy Lyapunov function [22, 25], to show that the proposed OFT controllers produce exponentially stable closed-loop systems. More specifically, our methodology is based on decomposing the closed-loop system into a slow and fast dynamics, and then the exponential stability of each dynamics is shown, which guarantees at the same time that the solution of the overall closed-loop dynamics vanishes exponentially.

Considering that OFT controllers can be more efficient than full-state feedback tracking controllers, specially if noisy velocity measurements are present, and taking

into account the philosophy of including saturation functions in an OFT control design, another contribution of this paper is an experimental comparison between OFT controllers that do not have saturation functions in its structure and controllers that do have saturation functions. The experiments were carried out in a two degrees-of-freedom direct-drive robot, which is important from the control point of view, because the dynamics the dynamics in this type of robots is highly nonlinear.

This paper is organized as follows. In Section 2 the robot dynamics and the control goal are discussed. Section 3 deals with the proposed class of OFT controllers and the closed-loop system analysis by using the stability theory of singularly perturbed systems. In Section 4, some design examples are provided. Section 5 is devoted to the experimental results, showing a comparison among several OFT controllers. Finally, some concluding remarks are given in Section 6.

Notation Throughout this paper the following notation will be adopted. $\|x\| = \sqrt{x^T x}$ stands for the norm of vector $x \in \mathbb{R}^n$. $\lambda_{\min}\{A(x)\}$ and $\lambda_{\max}\{A(x)\}$ denote the minimum and maximum eigenvalues of a symmetric positive definite matrix $A(x) \in \mathbb{R}^{n \times n}$ for all $x \in \mathbb{R}^n$, respectively. $\|B(x)\| = \sqrt{\lambda_{\max}\{B(x)^T B(x)\}}$ stands for the induced norm of a matrix $B(x) \in \mathbb{R}^{m \times n}$ for all $x \in \mathbb{R}^n$.

2 Robot Dynamics and Control Goal

The dynamics in joint space of a serial-chain n -link robot manipulator considering the presence of friction at the robot joints can be written as [2, 11, 18, 24],

$$M(q)\ddot{q} + C(q, \dot{q})\dot{q} + g(q) + F_v\dot{q} = \tau \tag{1}$$

where $M(q)$ is the $n \times n$ symmetric positive definite inertia matrix, $C(q, \dot{q})\dot{q}$ is the $n \times n$ vector of centripetal and Coriolis torques, $g(q)$ is the $n \times 1$ vector of gravitational torques, $F_v = \text{diag}\{f_{v1}, \dots, f_{vn}\}$ is the $n \times n$ positive definite diagonal matrix which contains the viscous friction coefficients of the robot joints, and τ is the $n \times 1$ vector of applied torque inputs

The following properties are satisfied for the dynamic model 1 – see e.g. [2, 11, 18, 24]: For robots with revolute joints, the vector of gravitational torques is bounded, i.e.,

$$k_g \geq \sup_{\forall q \in \mathbb{R}^n} \|g(q)\|. \tag{2}$$

For all $q, \dot{q}, x, y, z \in \mathbb{R}^n$, the inertia and Coriolis matrix (using Christoffel symbols) satisfy

$$C(x, y)z = C(x, z)y, \tag{3}$$

$$C(x, y + z) = C(x, y) + C(x, z), \tag{4}$$

$$\lambda_{\max}\{M(q)\}\|x\|^2 \geq x^T M(q)x \geq \lambda_{\min}\{M(q)\}\|x\|^2, \tag{5}$$

$$\dot{M}(q) = C(q, \dot{q}) + C(q, \dot{q})^T, \quad (6)$$

$$x^T \left[\frac{1}{2} \dot{M}(q) - C(q, \dot{q}) \right] x = 0, \quad (7)$$

$$\|C(q, \dot{q})\| \leq k_C \|\dot{q}\|, \quad k_C > 0. \quad (8)$$

Let \mathcal{T} denote the torque space, defined as

$$\mathcal{T} = \{\tau \in \mathbb{R}^n : -\tau_i^{\text{Max}} < \tau_i < \tau_i^{\text{Max}}, \quad i = 1, \dots, n\}, \quad (9)$$

with $\tau_i^{\text{Max}} > 0$ the maximum torque input for the i th joint. Assume that only robot joint displacements $q(t) \in \mathbb{R}^n$ are available for measurement and that the robot torque input is constrained to be at the torque space 9. Then, the OFT control problem is to design a control input $\tau(t) \in \mathcal{T}$ for all $t \geq 0$, so that the joint displacements $q(t) \in \mathbb{R}^n$ converge asymptotically to the desired joint displacements $q_d(t) \in \mathbb{R}^n$, i.e.,

$$\lim_{t \rightarrow \infty} \tilde{q}(t) = 0, \quad (10)$$

where

$$\tilde{q}(t) = q_d(t) - q(t) \quad (11)$$

denotes the tracking error. Throughout this paper we consider that $q_d(t)$ is two times differentiable and

$$\|\dot{q}_d(t)\| \leq \|\dot{q}_d\|_M, \quad \forall t \geq 0, \quad (12)$$

$$\|\ddot{q}_d(t)\| \leq \|\ddot{q}_d\|_M, \quad \forall t \geq 0, \quad (13)$$

where $\|\dot{q}_d\|_M > 0$ and $\|\ddot{q}_d\|_M > 0$ denote known constants.

3 A Class of OFT Controllers

We propose a class of OFT controllers which produces bounded torques:

$$\tau = M(q)\ddot{q}_d + C(q, \dot{q}_d)\dot{q}_d + g(q) + F_v\dot{q}_d + K_p\text{sat}(\tilde{q}) + K_d\text{sat}(\tilde{\dot{v}}), \quad (14)$$

where K_p and K_d are $n \times n$ positive definite diagonal matrices, the tracking error \tilde{q} is defined in Eq. 11, and the signal $\tilde{\dot{v}}$ is obtained from

$$\dot{q}_c = -b_f\text{sat}(\tilde{\dot{v}}), \quad (15)$$

$$\tilde{\dot{v}} = \dot{q}_c + b_f\tilde{q}, \quad (16)$$

with $b_f > 0$ and

$$\text{sat}(x) = [\text{sat}(x_1) \cdots \text{sat}(x_n)]^T, \quad \forall x \in \mathbb{R}^n.$$

P5 The gradient of the saturation function is strictly positive in the sense

$$\frac{\partial \text{sat}(x_i)}{\partial x_i} > 0, \forall x_i \in [-\eta, \eta] \subset \mathbb{R}, \tag{20}$$

where $\eta > 0$ and $i = 1, \dots, n$. The meaning of the inequality 20 is that the saturation function $\text{sat}(x_i)$, $x_i \in [-\eta, \eta]$, is a strictly increasing function. Notice that there are some saturation functions that satisfy the condition 20 in a global fashion, e.g., $\text{sat}(x_i) = \tanh(x_i)$, which satisfies

$$\frac{\partial \tanh(x_i)}{\partial x_i} = \text{sech}^2(x_i) > 0, \forall x_i \in \mathbb{R}.$$

The properties P1–P5 are mainly motivated by the analysis of the closed-loop system stability, as it will be seen later. An important observation is that the controller proposed in [15] (hereafter called Loría-Nijmeijer controller) is a particular case of the class of controllers 14, 15 and 16 using $\text{sat}(x_i) = \tanh(x_i)$.

The boundedness of the produced torque is assured with the assumption

$$\begin{aligned} & \max_{q \in \mathbb{R}^n} \{ \|M_i(q)\| \} \| \ddot{q}_d \|_M + \max_{q, \dot{q}_d \in \mathbb{R}^n} \{ \|C_i(q, \dot{q}_d)\| \} \| \dot{q}_d \|_M + \max_{q \in \mathbb{R}^n} \{ g_i(q) \} \\ & + f_{vi} | \dot{q}_{di} |_M + k_{di} b + k_{pi} b < \tau_i^{\text{Max}}, \quad i = 1, \dots, n, \end{aligned} \tag{21}$$

where b is involved in condition P1, $M_i(q)$ is the i th row of the inertia matrix $M(q)$, $C_i(q, \dot{q}_d)$ is the i th row of the matrix $C(q, \dot{q}_d)$, $g_i(q)$ the i th element of the vector $g(q)$, and $| \dot{q}_{di}(t) | \leq | \dot{q}_{di} |_M$ for all $t \geq 0$.

Substituting the controller 14 into the robot dynamics 1, using Eqs. 15 and 16 and the robot model properties 3 and 4 we obtain the closed-loop system

$$\frac{d}{dt} \begin{bmatrix} \tilde{q} \\ \dot{\tilde{q}} \end{bmatrix} = \begin{bmatrix} \dot{\tilde{q}} \\ -M(q)^{-1} [[C + C_d] \dot{\tilde{q}} + F_v \dot{\tilde{q}} + K_d \text{sat}(\tilde{\vartheta}) + K_p \text{sat}(\tilde{q})] \end{bmatrix}, \tag{22}$$

$$\epsilon \frac{d}{dt} \tilde{\vartheta} = -\text{sat}(\tilde{\vartheta}) + \dot{\tilde{q}}, \tag{23}$$

where $C = C(q, \dot{q})$, $C_d = C(q, \dot{q}_d)$, and

$$\epsilon = 1/b_f.$$

Note that for large numerical values of b_f the constant ϵ becomes small. The state space origin $[\tilde{q}^T \ \dot{\tilde{q}}^T \ \tilde{\vartheta}^T]^T = 0 \in \mathbb{R}^{3n}$ is the unique equilibrium point of the system 22 and 23, which has the form of a singularly perturbed system [12].

Roughly speaking, a singularly perturbed system can be decoupled in two subsystems: a slow dynamics subsystem and a fast dynamics subsystem. The exponential stability of each subsystem implies that the overall system is exponentially stable. This claim has been stated formally in Theorem 9.3 of [12], which, for the sake of completeness, is reproduced below. The notation B_r denotes the set given by the ball $\{ x \in \mathbb{R}^n : \|x\| \leq r \}$.

Theorem 1 Consider the singularly perturbed system

$$\dot{x} = f(t, x, z, \epsilon), \quad x \in \mathbb{R}^{n_1} \tag{24}$$

$$\epsilon \dot{z} = g(t, x, z, \epsilon), \quad z \in \mathbb{R}^{n_2}, \tag{25}$$

and $\epsilon > 0$. Assume that the following assumptions are satisfied for all

$$(t, x, \epsilon) \in [0, \infty) \times B_r \times [0, \epsilon_0]$$

- $f(t, 0, 0, \epsilon) = 0$ and $g(t, 0, 0, \epsilon) = 0$.
- The equation

$$0 = g(t, x, z, 0)$$

has an isolated root $z = h(t, x)$ such that $h(t, 0) = 0$.

- The functions f , g , and h and their partial derivatives up to order 2 are bounded for $z - h(t, x) \in B_\rho$.
- The origin of the reduced system

$$\dot{x} = f(t, x, h(t, x), 0) \tag{26}$$

is exponentially stable.

- The origin of the boundary-layer system

$$\frac{dy}{d\sigma} = g(t, x, y + h(t, x), 0), \tag{27}$$

$\sigma = t/\epsilon$, $y = z - h(t, x)$, is exponentially stable, uniformly in (t, x) .

Then, there exists $\epsilon^* > 0$ such that for all $\epsilon < \epsilon^*$, the origin of Eqs. 24 and 25 is exponentially stable.

Proof See [12], pag. 380. □

It is noteworthy that the subsystem 27 can be rewritten as

$$\frac{dz}{d\sigma} = g(t, x, z, 0), \tag{28}$$

which has equilibrium at $z^* = h(t, x)$. Then, exponential convergence of the limit

$$\lim_{\sigma \rightarrow \infty} z(\sigma) = z^* = h(t, x)$$

implies that $y(\sigma) \rightarrow 0$ as $\sigma \rightarrow \infty$ with exponential convergence rate also.

Now we are ready to introduce our results on the exponential stability of the closed-loop system 22 and 22.

Proposition 1 Assume that conditions P1–P5 are fulfilled and K_d is chosen so as to satisfy

$$\lambda_{\min}\{K_d\}k_{u0} + \lambda_{\min}\{F_v\}k_{u0}^2 - k_C\|\dot{q}_d\|_M k_{u1}^2 > 0 \tag{29}$$

with constants k_{u0} and k_{u1} defined in properties P1 and P3, respectively. Then, there always exists $\epsilon^* > 0$ such that for all $\epsilon^* > \epsilon > 0$, the state space origin of system 22 and 23 is locally exponentially stable.

Proof The exponential stability of the singularly perturbed system 22 and 23 is shown by invoking the Theorem 1. First, note that when $\epsilon = 0$ in Eqs. 22 and 23, the dimension of the state equation reduces from $3n$ to $2n$ because the differential equation 23 degenerates into the equation

$$0 = -\text{sat}(\tilde{\vartheta}) + \dot{\tilde{q}}. \tag{30}$$

The property P1 in Eq. 17 establishes that $|\text{sat}(x_i)| \leq b$. Thus, it is possible to restrict the stability analysis to some region of the state space where

$$|\dot{\tilde{q}}_i| \leq b_r < b, \quad i = 1, \dots, n,$$

where b_r is number that guarantees that Eq. 30 truly holds. Substituting Eq. 30 into Eq. 22 we obtain the reduced system – slow dynamics – given by

$$\frac{d}{dt} \begin{bmatrix} \tilde{q} \\ \dot{\tilde{q}} \end{bmatrix} = \begin{bmatrix} \dot{\tilde{q}} \\ -M(q)^{-1} [[C + C_d]\dot{\tilde{q}} + F_v\dot{\tilde{q}} + K_d\dot{\tilde{q}} + K_p\text{sat}(\tilde{q})] \end{bmatrix}, \tag{31}$$

which is a time-varying system and the state space origin $[\tilde{q}^T \ \dot{\tilde{q}}^T]^T = 0 \in \mathbb{R}^{2n}$ is its only equilibrium point. The exponential stability of the reduced model 31 can be shown through the following Lyapunov function

$$V(t, \tilde{q}, \dot{\tilde{q}}) = \frac{1}{2} \dot{\tilde{q}}^T M(q) \dot{\tilde{q}} + \sum_{i=1}^n k_{pi} \int_0^{\tilde{q}_i} \text{sat}(\tilde{q}_i) d\tilde{q}_i + \alpha \dot{\tilde{q}}^T M(q) \text{sat}(\tilde{q}) \tag{32}$$

where α is a small enough positive constant. By using the robot model property 5 and the right-hand side of property P4 in Eq. 19, it can be shown that under the condition

$$0 < \alpha < \alpha_1^*,$$

with small enough α_1^* , the function $V(t, \tilde{q}, \dot{\tilde{q}})$ is positive definite for all $[\tilde{q}^T \ \dot{\tilde{q}}^T]^T \in \Omega_r$,

$$\Omega_r = \left\{ \begin{bmatrix} \tilde{q} \\ \dot{\tilde{q}} \end{bmatrix} \in \mathbb{R}^{2n} : \|[\tilde{q}^T \ \dot{\tilde{q}}^T]^T\| \leq r \right\}, \tag{33}$$

with $r > 0$ the constant involved in the property P4.

The time derivative of $V(t, \tilde{q}, \dot{\tilde{q}})$ is given by

$$\begin{aligned} \dot{V}(t, \tilde{q}, \dot{\tilde{q}}) &= -\dot{\tilde{q}}^T C_d \dot{\tilde{q}} - \dot{\tilde{q}}^T F_v \dot{\tilde{q}} - \dot{\tilde{q}}^T K_d \text{sat}(\tilde{q}) - \alpha \text{sat}(\tilde{q})^T C_d \dot{\tilde{q}} - \alpha \text{sat}(\tilde{q})^T F_v \dot{\tilde{q}} \\ &\quad - \alpha \text{sat}(\tilde{q})^T K_d \text{sat}(\tilde{q}) - \alpha \text{sat}(\tilde{q})^T K_p \text{sat}(\tilde{q}) + \alpha \text{sat}(\tilde{q})^T C^T \dot{\tilde{q}} + \alpha \dot{\tilde{q}}^T M(q) \frac{\partial \text{sat}(\tilde{q})}{\partial \tilde{q}} \dot{\tilde{q}}, \end{aligned}$$

where the robot model properties 6 and 7 were used. By using properties P1–P3, the robot model property 8, and the inequality

$$\|\dot{\tilde{q}}\| \leq \|\dot{\tilde{q}}\| + \|\dot{q}_d\|_M,$$

$\|\dot{q}_d\|_M$ defined in Eq. 12, we can write an upper bound on $\dot{V}(t, \tilde{q}, \dot{\tilde{q}})$ as follows

$$\dot{V}(t, \tilde{q}, \dot{\tilde{q}}) \leq - \begin{bmatrix} \|\text{sat}(\tilde{q})\| \\ \|\text{sat}(\dot{\tilde{q}})\| \end{bmatrix}^T Q \begin{bmatrix} \|\text{sat}(\tilde{q})\| \\ \|\text{sat}(\dot{\tilde{q}})\| \end{bmatrix}, \tag{34}$$

where Q is a symmetric matrix with elements

$$\begin{aligned}
 Q_{11} &= \alpha \lambda_{\min}\{K_p\}, \\
 Q_{12} &= -\frac{1}{2}\alpha [2k_C \|\dot{q}_d\|_M k_{u1} + \lambda_{\max}\{K_d\} + \lambda_{\max}\{F_v\}k_{u1}k_{u0}], \\
 Q_{21} &= -\frac{1}{2}\alpha [2k_C \|\dot{q}_d\|_M k_{u1} + \lambda_{\max}\{K_d\} + \lambda_{\max}\{F_v\}k_{u1}k_{u0}], \\
 Q_{22} &= \lambda_{\min}\{K_d\}k_{u0}^2 + \lambda_{\min}\{F_v\}k_{u0}^2 - k_C \|\dot{q}_d\|_M k_{u1}^2 \\
 &\quad - \alpha [\sqrt{nb} k_C k_{u1}^2 + \beta k_{u1}^2 \lambda_{\max}\{M(q)\}].
 \end{aligned}$$

Inequality 34 is satisfied for all $[\tilde{q}^T \dot{\tilde{q}}^T]^T \in \Omega_r$ in Eq. 33.

By Sylvester’s theorem, the matrix Q in Eq. 34 is positive definite if condition 29 is satisfied and

$$0 < \alpha < \alpha_2^*,$$

with α_2^* small enough. The positive definiteness of Q implies that $\dot{V}(t, \tilde{q}, \dot{\tilde{q}})$ is negative definite for all $[\tilde{q}^T \dot{\tilde{q}}^T]^T \in \Omega_r$. Summarizing, for all $[\tilde{q}^T \dot{\tilde{q}}^T]^T \in \Omega_r$ we can always find a constant $0 < \alpha < \min\{\alpha_1^*, \alpha_2^*\}$ such that $V(t, \tilde{q}, \dot{\tilde{q}})$ is positive definite and $\dot{V}(t, \tilde{q}, \dot{\tilde{q}})$ is negative definite, implying the local asymptotic stability of the state space origin of the reduced system 31.

In addition, by using the left-hand side of property P4 in Eq. 19, we can claim that for $c_0 > 0$ large enough, the Lyapunov function $V(t, \tilde{q}, \dot{\tilde{q}})$ given in Eq. 32 attains the following upper bound

$$V(t, \tilde{q}, \dot{\tilde{q}}) \leq c_0 \left\| \begin{bmatrix} \|\text{sat}(\tilde{q})\| \\ \|\text{sat}(\dot{\tilde{q}})\| \end{bmatrix} \right\|^2, \tag{35}$$

for all $[\tilde{q}^T \dot{\tilde{q}}^T]^T \in \Omega_r$. Therefore, exponential stability comes from using inequalities 34 and 35 by writing

$$\dot{V}(t, \tilde{q}, \dot{\tilde{q}}) \leq -\frac{\lambda_{\min}\{Q\}}{c_0} V(t, \tilde{q}, \dot{\tilde{q}}),$$

which holds for all $[\tilde{q}^T \dot{\tilde{q}}^T]^T \in \Omega_r$.

On the other hand, the boundary layer model is

$$\frac{d}{d\sigma} \tilde{\vartheta} = -\text{sat}(\tilde{\vartheta}) + \dot{\tilde{q}} \tag{36}$$

where $\sigma = t/\epsilon$ and $\dot{\tilde{q}}$ is interpreted as a constant. Let us define the function

$$W(\tilde{\vartheta}_i) = \frac{1}{2} [\text{sat}(\tilde{\vartheta}_i) - \dot{\tilde{q}}_i]^2,$$

whose derivative with respect to the scaled time $\sigma = t/\epsilon$ is given by

$$\frac{d}{d\sigma} W(\tilde{\vartheta}_i) = -\frac{\partial \text{sat}(\tilde{\vartheta}_i)}{\partial \tilde{\vartheta}_i} [\text{sat}(\tilde{\vartheta}_i) - \dot{\tilde{q}}_i]^2. \tag{37}$$

Then, for a region $|\tilde{\vartheta}_i| \leq \eta$, in virtue of the property P5, we can define the constant

$$\bar{k} = \min_{\tilde{\vartheta}_i \in [-\eta, \eta]} \left\{ \frac{\partial \text{sat}(\tilde{\vartheta}_i)}{\partial \tilde{\vartheta}_i} \right\},$$

whereby Eq. 37 can be upper bounded as

$$\frac{d}{d\sigma} W(\tilde{\vartheta}_i) \leq -\bar{k}W(\tilde{\vartheta}_i),$$

which by the comparison lemma [12] implies that

$$[\text{sat}(\tilde{\vartheta}(\sigma)) - \dot{\tilde{q}}] \rightarrow 0$$

with exponential convergence rate as the scaled time $\sigma = t/\epsilon$ increases.

We have proven that the reduced model 31 and the boundary layer system 36 are locally exponentially stables. Then, by Theorem 1 in [12], there exists ϵ^* such that $\epsilon^* > \epsilon > 0$ guarantees local exponential stability of the closed-loop system 22 and 23 for some region of attraction. \square

Let us notice that by following the proof of Theorem 9.3 it can be shown that for $\epsilon^* > \epsilon > 0$ the set

$$R_A = \left\{ \begin{bmatrix} \tilde{q} \\ \dot{\tilde{q}} \\ \tilde{\vartheta} \end{bmatrix} \in \mathbb{R}^{3n} : \left\| \begin{bmatrix} \tilde{q} \\ \dot{\tilde{q}} \\ \tilde{\vartheta} \end{bmatrix} \right\| < \min\{b_r, \eta\} \right\},$$

with $b_r < b$, the constant b defined in Eq. 17, and $\eta > 0$ related to property P5 in Eq. 20, is a region of attraction in which the exponential stability of the system 22 and 23 is guaranteed.

4 Some Design Examples

4.1 Design 1

Consider the saturation function

$$\text{sat}(x_i) = \frac{x_i}{\sqrt{\delta_i + x_i^2}}, \tag{38}$$

where $\delta_i > 0$. The controller generated with this saturation function is given by

$$\begin{aligned} \tau = & M(q)\ddot{q}_d + C(q, \dot{q}_d)\dot{q}_d + g(q) + F_v\dot{q}_d + K_d \text{col} \left\{ \frac{\tilde{\vartheta}_i}{\sqrt{\delta_{di} + \tilde{\vartheta}_i^2}} \right\} \\ & + K_p \text{col} \left\{ \frac{\tilde{q}_i}{\sqrt{\delta_{pi} + \tilde{q}_i^2}} \right\}, \end{aligned} \tag{39}$$

where $\text{col}\{x_i\} = [x_1 \ \dots \ x_n]^T \in \mathbb{R}^n$, and the subindex p or d of the parameter δ_i in Eq. 38 denotes the relation to the proportional or derivative part of the controller.

The conditions P1–P5 are verified as follows:

- **P1** We can select $b = 1$ and $k_{u0} = 1$ to verify that equations related to property P1 are satisfied.
- **P2** This condition is related to the upper bound of the gradient of the saturation function 38, i.e.,

$$\frac{\partial}{\partial x_i} \frac{x_i}{\sqrt{\delta_i + x_i^2}} = -\frac{x_i^2}{[\delta_i + x_i^2]^{3/2}} + \frac{1}{\sqrt{\delta_i + x_i^2}} \leq 1/\sqrt{\delta_i}, \forall x_i \in \mathbb{R}.$$

Then, we can select $\beta = \max_i\{1/\sqrt{\delta_i}\}$.

- **P3** For the region $|x_i| \leq r$, the inequality

$$|x_i| \leq k_{u1i} \frac{|x_i|}{\sqrt{\delta_i + x_i^2}}$$

is attained using $k_{u1i} \geq \sqrt{\delta_i + r^2}$, so that $k_{u1} = \max_i\{k_{u1i}\}$.

- **P4** This property can be explicitly written as

$$k_{u2i} \frac{x_i^2}{\delta_i + x_i^2} \geq \sqrt{\delta_i + x_i^2} - \sqrt{\delta_i} \geq k_{u3i} \frac{x_i^2}{\delta_i + x_i^2},$$

which should be satisfied for the region $|x_i| \leq r$, which is accomplished with

$$k_{u2i} \geq \frac{[\delta_i + r^2][\sqrt{\delta_i + r^2} - \sqrt{\delta_i}]}{r^2},$$

and

$$k_{u3i} \leq \lim_{r \rightarrow 0} \frac{[\delta_i + r^2][\sqrt{\delta_i + r^2} - \sqrt{\delta_i}]}{r^2} = \frac{\sqrt{\delta_i}}{2},$$

which is obtained by using the L'Hôpital's rule. Then, $k_{u2} = \max_i\{k_{u2i}\}$ and $k_{u3} = \min_i\{k_{u3i}\}$.

- **P5** The gradient of the saturation function 38 is given by

$$\frac{\partial}{\partial x_i} \text{sat}(x_i) = -\frac{x_i^2}{[\delta_i + x_i^2]^{3/2}} + \frac{1}{\sqrt{\delta_i + x_i^2}}.$$

By solving the inequality

$$-\frac{x_i^2}{[\delta_i + x_i^2]^{3/2}} + \frac{1}{\sqrt{\delta_i + x_i^2}} > 0$$

we found that the condition P5 is satisfied for all $x_i \in \mathbb{R}$.

4.2 Design 2

A second design is provided through the saturation function

$$\text{sat}(x_i) = \frac{x_i}{\delta_i + \ln(\cosh(x_i))} \tag{40}$$

where $\delta_i > 0$. Then, the generated controller is given by

$$\begin{aligned} \tau = & M(q)\dot{q}_d + C(q, \dot{q}_d)\dot{q}_d + g(q) + F_v\dot{q}_d + K_d \text{col} \left\{ \frac{\tilde{\vartheta}_i}{\delta_{di} + \ln(\cosh(\tilde{\vartheta}_i))} \right\} \\ & + K_p \text{col} \left\{ \frac{\tilde{q}_i}{\delta_{pi} + \ln(\cosh(\tilde{q}_i))} \right\}, \end{aligned} \tag{41}$$

where, like in the new controller 39, we have used the notation $\text{col}\{x_i\} = [x_1 \ \cdots \ x_n]^T \in \mathbb{R}^n$, and the subindex p or d of the parameter δ_i in Eq. 40 denotes the relation to the proportional or derivative part of the controller.

Similarly to the previous subsection, the conditions P1–P5 are first verified for the scalar case 40, and then extended to the vector case:

- **P1** The saturation function 40 satisfies this condition. Namely, for any δ_i , we can find a proper constant b so that $|\text{sat}(x_i)| \leq b$, for all $x_i \in \mathbb{R}$. Besides, the condition

$$\frac{x_i^2}{\delta_i + \ln(\cosh(x_i))} \geq k_{u0i} \frac{x_i^2}{[\delta_i + \ln(\cosh(x_i))]^2}$$

is satisfied for all $x_i \in \mathbb{R}$ using $k_{u0i} \leq \delta_i$; thus $k_{u0} = \min_i\{k_{u0i}\}$.

- **P2** In this condition we have that

$$\begin{aligned} \frac{\partial}{\partial x_i} \frac{x_i}{\delta_i + \ln(\cosh(x_i))} &= - \frac{x_i \tanh(x_i)}{[\delta_i + \ln(\cosh(x_i))]^2} \\ &+ \frac{1}{\delta_i + \ln(\cosh(x_i))} \leq 1/\delta_i, \quad \forall x_i \in \mathbb{R}. \end{aligned}$$

Therefore, $\beta = \max_i\{1/\delta_i\}$.

- **P3** In a similar form to the case of the saturation function 38, for the region $|x_i| \leq r$, the inequality

$$|x_i| \leq k_{u1i} \frac{|x_i|}{\delta_i + \ln(\cosh(x_i))}$$

is attained using $k_{u1i} \geq \delta_i + \ln(\cosh(r))$. Hence $k_{u1} = \max_i\{k_{u1i}\}$.

- **P4** This property consists in satisfying

$$k_{u2i} \frac{x_i^2}{[\delta_i + \ln(\cosh(x_i))]^2} \geq f(x_i) \geq k_{u3i} \frac{x_i^2}{[\delta_i + \ln(\cosh(x_i))]^2},$$

with $f(x_i) = \int_0^{x_i} \frac{x_i}{\delta_i + \ln(\cosh(x_i))} dx_i$, for the region $|x_i| \leq r$. This is accomplished with

$$k_{u2i} \geq \frac{[\delta_i + \ln(\cosh(r))]^2}{r^2} f(r).$$

and

$$k_{u3i} \leq \lim_{r \rightarrow 0} \frac{[\delta_i + \ln(\cosh(r))]^2}{r^2} f(r) = \frac{\delta_i}{2},$$

which is obtained by using the L'Hôpital's rule. Then, $k_{u2} = \max_i \{k_{u2i}\}$ and $k_{u3} = \min_i \{k_{u3i}\}$.

- **P5** This consists in that

$$\frac{\partial \text{sat}(x_i)}{\partial x_i} = -\frac{x_i \tanh(x_i)}{[\delta + \ln(\cosh(x_i))]^2} + \frac{1}{\delta + \ln(\cosh(x_i))} > 0$$

for all $x_i \in [-\eta, \eta]$. Solving this inequality, we obtain

$$\delta + \ln(\cosh(x_i)) > x_i \tanh(x_i),$$

which clearly holds for all $x_i \in [-\eta, \eta]$. Then, the saturation function 40 satisfies the condition P5.

5 Experimental Results

A direct-drive arm with two vertical rigid links – see Fig. 2 – is available at the Control Laboratory of the *Instituto Tecnológico de La Laguna*, which was designed and built at the Robotics Laboratory of CICESE Research Center. High-torque, brushless direct-drive motors operating in torque mode are used to drive the joints without gear reduction.

A motion control board based on a TMS320C31 32-bit floating-point microprocessor from Texas Instruments is used to execute the control algorithm. The control program is written in C programming language executed in the control board at $h = 2.5$ [ms] sampling period. The maximum torque limits are $\tau_1^{\text{Max}}=150$ [Nm] and $\tau_2^{\text{Max}}=15$ [Nm] for motor 1 and 2, respectively.

Fig. 2 Experimental robot arm



Table 1 Parameters of the manipulator

	Notation	Value	Unit
Link 1 length	l_1	0.45	m
Link 2 length	l_2	0.45	m
Link 1 center of gravity	l_{c1}	0.091	m
Link 2 center of gravity	l_{c2}	0.048	m
Link 1 mass	m_1	23.90	kg
Link 2 mass	m_2	3.88	kg
Link 1 inertia	I_1	1.27	kg m ²
Link 2 inertia	I_2	0.09	kg m ²
Gravity acceleration	g	9.8	m/s ²

With reference to the symbols listed in Table 1, we present below the entries of the robot dynamics [20, 21]:

The elements $M_{ij}(q)$ ($i, j = 1, 2$) of the inertia matrix $M(q)$ are

$$M_{11}(q) = m_1 l_{c1}^2 + m_2 (l_1^2 + l_{c2}^2 + 2l_1 l_{c2} \cos(q_2)) + I_1 + I_2,$$

$$M_{12}(q) = m_2 (l_{c2}^2 + l_1 l_{c2} \cos(q_2)) + I_2,$$

$$M_{21}(q) = m_2 (l_{c2}^2 + l_1 l_{c2} \cos(q_2)) + I_2,$$

$$M_{22}(q) = m_2 l_{c2}^2 + I_2.$$

The elements $C_{ij}(q, \dot{q})$ ($i, j = 1, 2$) from the centrifugal and Coriolis matrix $C(q, \dot{q})$ are

$$C_{11}(q, \dot{q}) = -m_2 l_1 l_{c2} \sin(q_2) \dot{q}_2,$$

$$C_{12}(q, \dot{q}) = -m_2 l_1 l_{c2} \sin(q_2) (\dot{q}_1 + \dot{q}_2),$$

$$C_{21}(q, \dot{q}) = m_2 l_1 l_{c2} \sin(q_2) \dot{q}_1,$$

$$C_{22}(q, \dot{q}) = 0.$$

The entries of the gravitational torque vector $g(q)$ are given by

$$g_1(q) = (m_1 l_{c1} + m_2 l_1) g \sin(q_1) + m_2 l_{c2} g \sin(q_1 + q_2),$$

$$g_2(q) = m_2 l_{c2} g \sin(q_1 + q_2).$$

The coefficients of the viscous friction are

$$F_v = \text{diag}\{2.288, 0.175\} \text{ [N m s]}.$$

Experiments showed that static and Coulomb friction at the motor joints are present and they depend in a complex manner on the joint position and velocity. We have decided to consider them as disturbances for the closed-loop system.

5.1 Desired Position Trajectory and Performance Criterion

The desired position trajectory $q_d(t)$ used in all experiments is given by

$$q_d(t) = \begin{bmatrix} 45[1 - e^{-2.0t^3}] + 10[1 - e^{-2.0t^3}] \sin(7.50t) \\ 60[1 - e^{-1.8t^3}] + 125[1 - e^{-1.8t^3}] \sin(1.75t) \end{bmatrix} \text{ [degrees]} \quad (42)$$

With regard to the desired joint position 42, it is easy to show that its components satisfy $\|\dot{q}_d(t)\| \leq \|\dot{q}_d\|_M$ and $\|\ddot{q}_d(t)\| \leq \|\ddot{q}_d\|_M$ for all $t \geq 0$.

An important characteristic of the position trajectory $q_d(t)$ in Eq. 42 is that the desired velocity $\dot{q}_d(t)$ and acceleration $\ddot{q}_d(t)$ are nulls in $t = 0$, then the closed-loop system trajectories will not present rude transients if the robot starts at rest. It is noteworthy that the execution of the proposed trajectory $q_d(t)$ in Eq. 42 demanded a 75% of the torque capabilities, which was estimated through numerical simulation and verified with the experiments.

The time evolution of the position error \tilde{q} reflects how well the control system performance is. The performance criterion considered in this paper was the root mean square – RMS – value of the velocity error computed on a trip of time T , that is,

$$\text{RMS}[\dot{\tilde{q}}] = \sqrt{\frac{1}{T} \int_0^T \|\dot{\tilde{q}}(\sigma)\|^2 d\sigma} \text{ [degrees/s]}. \quad (43)$$

In practice, the discrete implementation of the criterion 43 leads to

$$\text{RMS}[\dot{\tilde{q}}] = \sqrt{\frac{1}{T} \sum_{k=0}^i \|\dot{\tilde{q}}(kh)\|^2 h} \text{ [degrees/s]},$$

where $h = 2.5$ [ms] is the sampling period and $T = 10$ [s].

5.2 Tested Controllers

We have tested six controllers with the aim of evaluating the performance of the proposed class of OFT tracking controllers. Three of the tested controllers do not contain saturation functions, while the others do it. The main goal of the experimental evaluation was to assess the tracking performance of controllers that do not have saturation functions,

- PD+ [19],
- Loría and Ortega [14], and
- Lee and Khalil [13],

with respect to those that have saturation functions,

- Loría and Nijmeijer [15],
- New Design in Eq. 39, and
- New Design in Eq. 41.

Let us first describe the results concerning controllers without saturation functions. The first controller tested was the PD+ control [19], which is written as

$$\tau = M(q)\ddot{q}_d + C(q, \dot{q})\dot{q}_d + g(q) + F_v\dot{q} + K_d\dot{\tilde{q}} + K_p\tilde{q}, \quad (44)$$

where $\tilde{q} = q_d - q$ denotes the tracking error and the joint velocity measurements \dot{q} are approached via simple numerical differentiation, i.e.,

$$\dot{q}_i(hk) = \frac{q_i(hk) - q_i(h[k-1])}{h} \quad (45)$$

where h is the sampling period and k is the discrete time. It is well known that the approach 45 is very common in many robot control platforms to obtain an estimation of the velocity measurements. The controller was tested using the following proportional and derivative control gains

$$\begin{aligned} K_p &= \text{diag}\{3500, 1000\} [1/s^2], \\ K_d &= \text{diag}\{45, 15\} [1/s], \end{aligned} \quad (46)$$

Let us notice that the gains 46 were obtained by trial and error until obtaining a reasonable performance in the tracking of the desired joint position $q_d(t)$, i.e., a relatively small enough bound of the maximum values of $\tilde{q}_1(t)$ and $\tilde{q}_2(t)$. The Fig. 3 shows the time evolution of tracking errors $\tilde{q}_1(t)$, $\tilde{q}_2(t)$, and applied torques $\tau_1(t)$, $\tau_2(t)$.

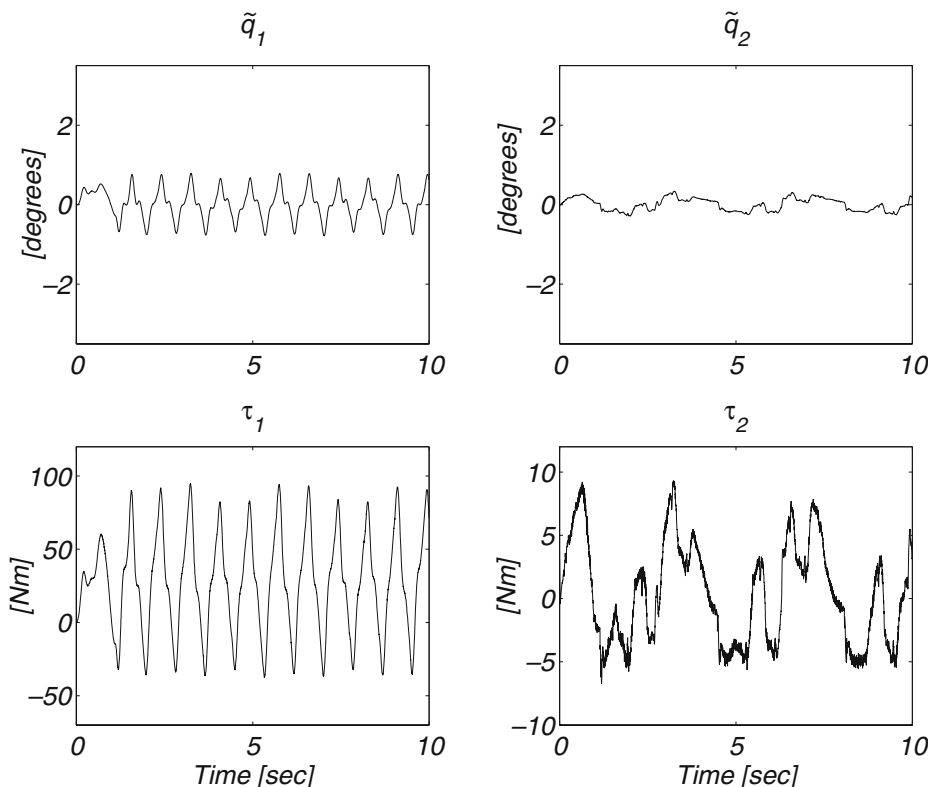


Fig. 3 PD+ controller : Tracking errors $\tilde{q}_1(t)$, $\tilde{q}_2(t)$, and applied torques $\tau_1(t)$, $\tau_2(t)$

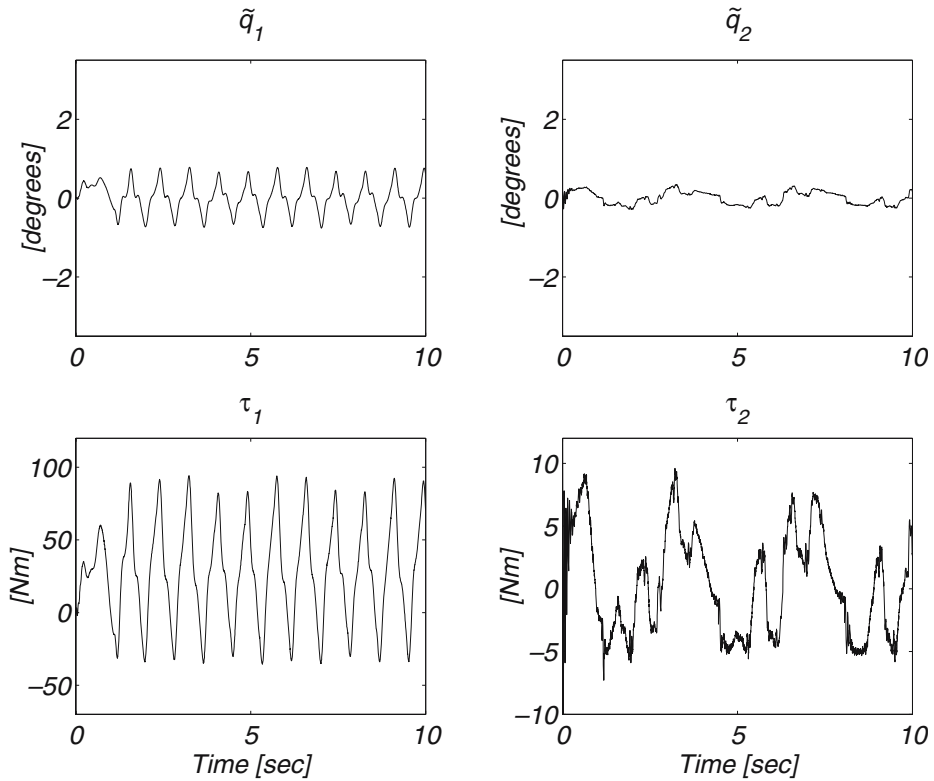


Fig. 4 Loría and Ortega controller: Tracking errors $\tilde{q}_1(t)$, $\tilde{q}_2(t)$, and applied torques $\tau_1(t)$, $\tau_2(t)$

Further improvement could have been obtained in the tracking performance, but paying the price of a noisy control action which would excite other dynamics such as vibrating modes of the mechanical structure.

Since all the controllers have a proportional-derivative structure, we have used the same numerical value of the gains in Eq. 46, while the gain of the filter used in each controller was selected until a reasonable performance was obtained, as we will explain later.

The other two control schemes that do not contain saturation functions correspond to the OFT controllers by Loría and Ortega [14] and Lee and Khalil [13]. The Loría and Ortega controller [14] is written as

$$\tau = M(q)\ddot{q}_d + C(q, \dot{q}_d)\dot{q}_d + g(q) + F_v\dot{q} + K_d\tilde{\vartheta} + K_p\tilde{q}, \tag{47}$$

where $\tilde{\vartheta} \in \mathbb{R}^n$ is obtained with the linear filter

$$\begin{aligned} \dot{x} &= -b_f\tilde{\vartheta}, \\ \tilde{\vartheta} &= x + b_f\tilde{q}. \end{aligned}$$

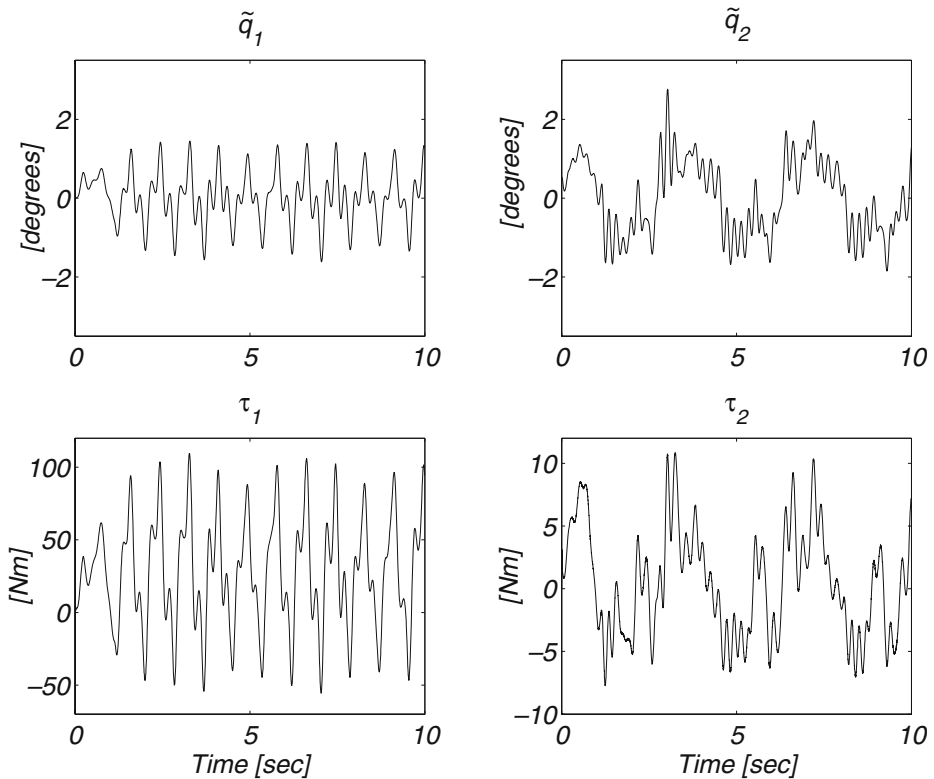


Fig. 5 Lee and Khalil controller: Tracking errors $\tilde{q}_1(t)$, $\tilde{q}_2(t)$, and applied torques $\tau_1(t)$, $\tau_2(t)$

The controller 47 was implemented in our system with the control gains 46 and

$$b_f = 600.0 \text{ [1/s]}. \tag{48}$$

The Lee and Khalil controller [13] in its non adaptive version can be written as

$$\tau = M(q_d - x_1)\ddot{q}_d + C(q_d - x_1, \dot{q}_r)\dot{q}_d + g(q_d - x_1) + F_v[\dot{q}_d - x_2] + K_d x_2 + K_p x_1, \tag{49}$$

where $\dot{q}_r = \dot{q}_d - x_2 + \lambda \tilde{q}$ and the second order high-gain observer

$$\dot{x}_1 = x_2 + \frac{L_1}{\epsilon}[\tilde{q} - x_1], \tag{50}$$

$$\begin{aligned} \dot{x}_2 = & \frac{L_2}{\epsilon^2}[\tilde{q} - x_1] + \ddot{q}_d + M(q_d - x_1)^{-1}[C(q_d - x_1, \dot{q}_r)\dot{q}_d \\ & + g(q - x_1) + F_v[\dot{q}_d - x_2] - \tau]. \end{aligned} \tag{51}$$

The gains used for the implementation of this controller were K_p and K_v in Eq. 46, $\lambda = 1 \text{ [1/s]}$,

$$L_1 = \text{diag}\{5.0, 40.0\} \text{ [1/s]}, \quad L_2 = \text{diag}\{50, 400.0\} \text{ [1/s}^2\text{]},$$

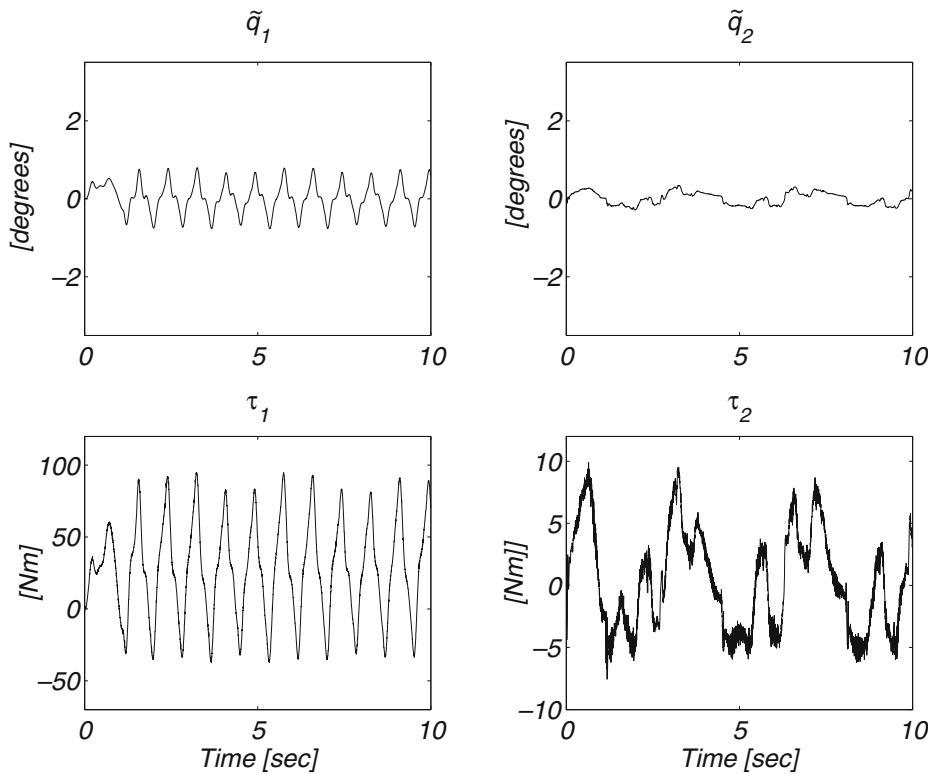


Fig. 6 Loría and Nijmeijer controller: Tracking errors $\tilde{q}_1(t)$, $\tilde{q}_2(t)$, and applied torques $\tau_1(t)$, $\tau_2(t)$

and $\epsilon = 0.1$ [dimensionless]. We tried several sets of gains for the observer 50 and 51 until obtaining a good response in the tracking error. However, it was pretty difficult to find numerical values for which instability was avoided. As pointed out in [3], the real-time implementation of the controller/observer 49–51 may make estimations of the position and velocity errors inaccurate to the point of not being useful and instable, which was confirmed in the experimental set up.

The obtained experimental results are given in Fig. 4, for the Loría and Ortega controller, and in Fig. 5, for the Lee and Khalil scheme.

On other hand, concerning OFT controllers that contain saturation functions in its structure, the first controller tested was the Loría and Nijmeijer approach [15] written as

$$\tau = M(q)\ddot{q}_d + C(q, \dot{q}_d)\dot{q}_d + g(q) + F_v\dot{q} + K_d \tanh(\tilde{\vartheta}) + K_p \tanh(\tilde{q}), \quad (52)$$

used along with the saturated filter

$$\dot{x} = -b_f \tanh(\tilde{\vartheta}), \quad (53)$$

$$\tilde{\vartheta} = x + b_f \tilde{q}. \quad (54)$$

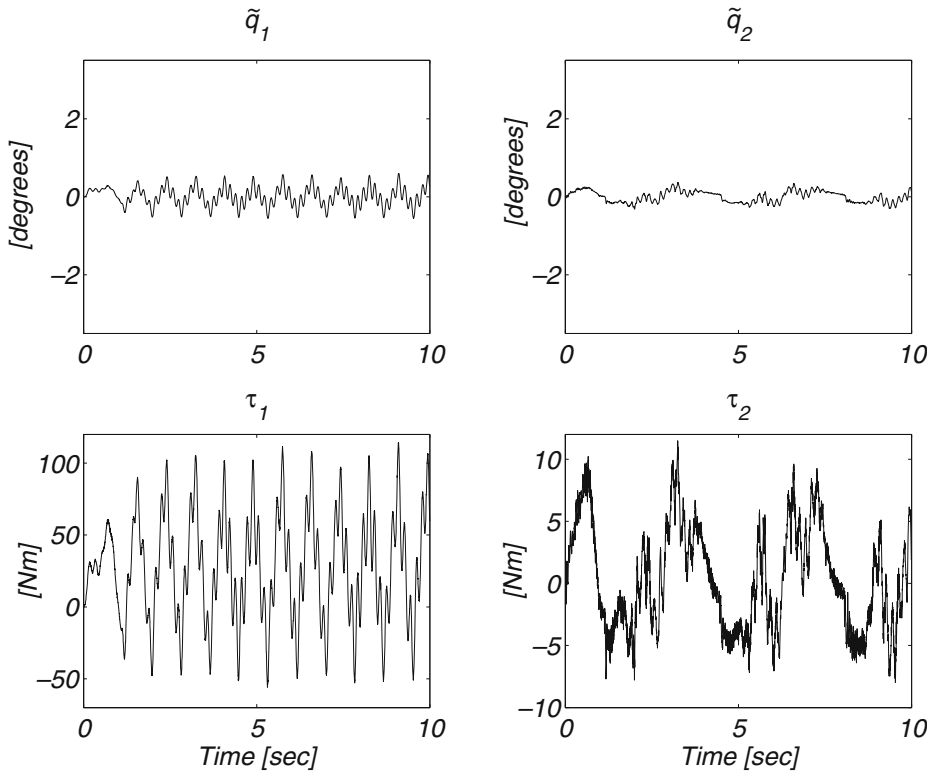


Fig. 7 New Design 1: Tracking errors $\tilde{q}_1(t)$, $\tilde{q}_2(t)$, and applied torques $\tau_1(t)$, $\tau_2(t)$

Note that Loría and Nijmeijer approach (Eqs. 52–54) is a particular case of the class of controllers 14–16 using $\text{sat}(x_i) = \tanh(x_i)$. Once again, in order to keep a fair comparison with respect to the three previous controllers that do not use saturation functions, we used the numerical values of K_p and K_d in Eq. 46 and b_f in Eq. 48. The result of the experiment is depicted in Fig. 6.

Besides, we implemented the controller denoted as New Design 1, in Eq. 39, which is derived from the proposed class of controller 14–16. Similarly, we chose the numerical values of K_p and K_d as in Eq. 46, and b_f as in Eq. 48. Parameters δ_i corresponding to the saturation function 38 were

$$\delta_{p1} = 0.3, \delta_{p2} = 0.75, \delta_{d1} = 1.0, \delta_{d2} = 1.0.$$

Figure 7 shows the results of the experiment.

Finally, the controller New Design 2, in Eq. 41, was tested under the same conditions that the New Design 1, while the parameters δ_i used in this case were

$$\delta_{p1} = 0.55, \delta_{p2} = 1.0, \delta_{d1} = 1.0, \delta_{d2} = 1.0.$$

The results are illustrated in Fig. 8.

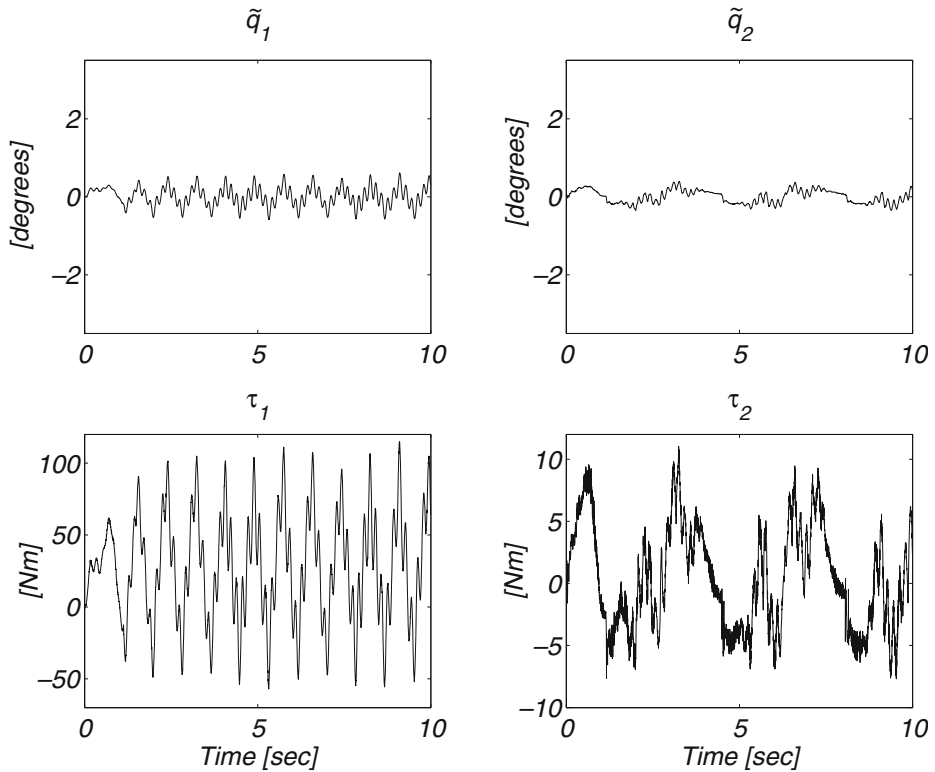


Fig. 8 New Design 2: Tracking errors $\tilde{q}_1(t)$, $\tilde{q}_2(t)$, and applied torques $\tau_1(t)$, $\tau_2(t)$

5.3 Discussions

All the tested controllers assure theoretically that the position error $\tilde{q}(t)$ must vanish as time increases. In practice, Figs. 3–8 reveal an steady state oscillatory behavior. This is due to several factors such as uncompensated Coulomb friction and discrete controller implementation.

Table 2 summarizes the information about the tracking performance of the six schemes, remarking the difference between controllers that do not use saturation functions and controllers that do use them. In addition, Fig. 9 shows a bar chart of the $RMS[\tilde{q}]$ value computed for the six tested controllers. With respect to controllers without saturation function we can see that the performance of the PD+ controller 44 and the Loría and Ortega algorithm (Eq. 47) is very similar, while the worst performance of the six controllers was obtained with Lee and Khalil controller 49. On the other hand, concerning the experimental results using controllers with saturation function, we can see that the performance of the Loría and Nijmeijer scheme 52 is very similar to the one of the controllers PD+ (Eq. 44) and Loría and Ortega (Eq. 47). The reason is that in the situation of a very small tracking error \tilde{q} the structure of the three controllers is very similar. In addition, the best performance of the six controllers was obtained with the New Design 1 and New Design 2 in Eqs. 39 and 41, respectively, because they presented the lowest values of $\max\{|\tilde{q}_1(t)|\}$, $\max\{|\tilde{q}_2(t)|\}$

Table 2 Performance of the controllers: PD+, Loría and Ortega (LO), Lee and Khalil (LK), Loría and Nijmeijer (LN), New Design 1, and New Design 2

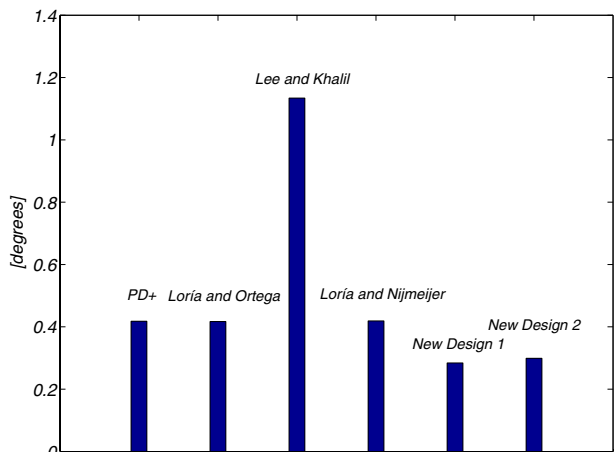
	Controllers without saturation functions			Controllers with saturation functions		
	PD+	LO	LK	LN	New 1	New 2
$\max\{ \tilde{q}_1(t) \}$ [deg]	0.78	0.75	1.62	0.79	0.59	0.61
$\max\{ \tilde{q}_2(t) \}$ [deg]	0.34	0.34	2.76	0.34	0.36	0.39
RMS $[\tilde{q}]$ [deg]	0.418	0.417	1.134	0.419	0.284	0.299

and RMS $[\tilde{q}]$. This is also appreciated in the Fig. 9, which depicts the bar chart of the RMS $[\tilde{q}]$ value.

The comparison reveals that all the controllers work efficiently since the tracking errors are relatively close to the performance of the PD+ controller 44, although the proposed controllers 39 and 41, which incorporate saturation functions, present the lowest tracking error $\tilde{q}(t)$ than other OFT controllers, including the PD+ control 44. The explanation of this is that the new controllers 39 and 41 incorporate the extra parameters δ_{pi} , δ_{di} , whose numerical value has effect in increasing the slope of the profile of the saturation function in the proximity of the origin. Different numerical values of δ_i lead to a similar behavior with respect to the PD+ (Eq. 44), Loría and Ortega (Eq. 47), and Loría and Nijmeijer (Eq. 52) schemes.

6 Concluding Remarks

In this paper the OFT (output feedback tracking) control of robot manipulators subject to constrained torques was studied. In particular, a class of controllers was proposed whose exponential stability proof was based on the theory of singularly perturbed system, which has been recognized as a powerful tool in robot dynamics and control. An extensive experimental study in a two degrees-of-freedom direct-

Fig. 9 Bar chart of the RMS $[\tilde{q}]$ value computed for the six tested controllers

drive robot was presented, where it was shown that torque-saturated OFT controllers present better tracking performance than the non-saturated counterpart. To the best of the authors' knowledge, the six OFT controllers discussed in the experimental results have been tested in a real-time robot control system for the first time. The results obtained in practice suggest that the application of torque-saturated OFT controllers in industrial robots is reliable.

Acknowledgements This work is partially supported by DGEST, CONACyT, Mexico, grants 60230 and 52174, and SIP-IPN.

References

1. Arteaga, M.A.: Robot control and parameter estimation with only joint position measurements. *Automatica* **39**, 67–73 (2003)
2. Canudas de Wit, C., Siciliano, B., Bastin, G. (eds.): *Theory of Robot Control*. Springer, London (1996)
3. Daly, J.M., Schwartz, H.M.: Experimental results for output feedback adaptive robot control. *Robotica* **24**, 727–738 (2006)
4. Dixon, W.E., de Queiroz, M.S., Dawson, D.M., Zhang, F.: Tracking control of robot manipulators with bounded torque inputs. In: *Proc. of the IASTED International Conference on Robotics and Manufacturing*, pp. 112–115. Banff, Canada, July (1998)
5. Dixon, W.E., de Queiroz, M.S., Zhang, F., Dawson, D.M.: Tracking control of robot manipulators with bounded torque input. *Robotica* **17**, 121–129 (1999)
6. Dixon, W.E., Zergeroglu, E., Dawson, D.M.: Global robust output feedback tracking control of robot manipulators. *Robotica* **22**(4), 351–357 (2004)
7. Dixon, W.E.: Adaptive regulation of amplitude limited robot manipulators with uncertain kinematics and dynamics. *IEEE Trans. Automat. Contr.* **52**(3), 488–493 (2007)
8. Glatfelder, A.H., Schaufelberger, W.: *Control Systems with Input and Output Constraints*. Springer, London (2003)
9. Hu, T., Lin, Z.: *Control Systems with Actuator Saturation: Analysis and Design*. Birkhauser, Boston (2001)
10. Kapila, V., Grigoriadis, K.M. (eds.): *Actuator Saturation Control*. Marcel Dekker, New York (2002)
11. Kelly, R., Santibáñez, V., Loria, A.: *Control of Robot Manipulators in Joint Space*. Springer, Berlin (2005)
12. Khalil, H.: *Nonlinear Systems*. Prentice-Hall, Upper Saddle River (1996)
13. Lee, K.W., Khalil, H.: Adaptive output feedback control of robot manipulators using high-gain observer. *Int. J. Control* **67**(6), 869–886 (1997)
14. Loria, A., Ortega, R.: On tracking control of rigid and flexible joint robots. *Appl. Math. Comput. Sci.* **5**(2), 329–341 (1995)
15. Loria, A., Nijmeijer, H.: Bounded output feedback tracking control of full actuated Euler–Lagrange systems. *Syst. Control. Lett.* **33**, 151–161 (1998)
16. Meza, J.L., Santibáñez, V., Hernández, V.M.: Saturated nonlinear PID global regulator for robot manipulators: passivity based analysis. In: *Proc. of 16th IFAC World Congress*, pp. 3–8. Prague, July (2005)
17. Melhem, K., Liu, Z., Loria, A.: A unified framework for dynamics and Lyapunov stability of holonomically constrained rigid bodies. *Journal of Advanced Computational Intelligence and Intelligent Informatics* **9**, 387–394 (2005)
18. Ortega, R., Loria, A., Nicklasson, P.J., Sira-Ramirez, H.: *Passivity-Based Control of Euler–Lagrange Systems*. Springer, London (1998)
19. Paden, B., Panja, R.: Globally asymptotically stable PD+ controller for robot manipulators. *Int. J. Control* **7**(6), 1697–1712 (1988)
20. Reyes, F., Kelly, R.: Experimental evaluation of identification schemes on a direct drive robot. *Robotica* **15**, 563–571 (1997)
21. Reyes, F., Kelly, R.: Experimental evaluation of model-based controllers on a direct-drive robot arm. *Mechatronics* **11**, 267–282 (2001)

22. Santibáñez, V., Kelly, R.: Strict Lyapunov functions for control of robot manipulators. *Automatica* **33**(4), 675–682 (1997)
23. Santibáñez, V., Kelly, R.: Global asymptotic stability of bounded output feedback tracking control for robot manipulators. In: 40th IEEE Conf. Decision and Control, pp. 1378–1379. Orlando, December (2001)
24. Sciavicco, L., Siciliano, B.: *Modeling and Control of Robot Manipulators*. Springer, London (2000)
25. Takegaki, M., Arimoto, S.: A new feedback method for dynamic control of manipulators. *ASME J. Dyn. Syst. Meas. Control* **103**, 119–125 (1981)
26. Zavala-Río, A., Santibáñez V.: Simple extensions of the PD-with-gravity-compensation control law for robot manipulators with bounded inputs. *IEEE Trans. Control Syst. Technol.* **14**(5), 958–965 (2006)
27. Zavala-Río, A., Santibáñez V.: A natural saturating extension of the PD-control-with-desired-gravity-compensation for robot manipulators with bounded inputs. *IEEE Trans. Robot. Autom.* **23**(2), 386–391 (2007)
28. Zergeroglu, E., Dawson, D.M., de Queiroz, M.S., Krstić, M.: On global output feedback tracking control of robot manipulators. In: Proc. of the IEEE Conference on Decision and Control, pp. 5073–5078. Sydney, Australia (2000)
29. Zergeroglu, E., Dixon, W.E., Behal, A., Dawson: Adaptive set-point control of robotic manipulators with amplitude-limited control inputs. *Robotica* **18**(2), 171–181 (2000)